Dislocation Patterns in Strained Layers from Sources on Parallel Glide Planes

K. W. Schwarz and F. K. LeGoues
IBM Watson Research Center, P.O. Box 218, Yorktown Heights, New York 10598
(Received 27 May 1997)

The interaction of dislocations on parallel glide planes in a strained epitaxial layer is investigated nu-merically. It is found that if two dislocations approach closely enough they will form an immobile bound complex. If a third dislocation now comes near such a complex, it will knock one of the partners forward and in turn bind with the survivor. The repetitive action of this simple process leads to the growth of elaborate network structures in the substrate. The network geometry predicted by the calculation is remarkably similar to previously unexplained dislocation structures observed in transmission electron microscopy images. [S0031-9007(97)03990-2]

PACS numbers: 61.72.Lk, 68.55.Ln

The growth of thin epitaxial layers on a crystalline substrate such as silicon is a process of considerable importance in the manufacture of semiconducting heterostructures and devices. Since the equilibrium lattice constant of the layer material (here $Si_{1-x}Ge_x$) differs from that of the substrate, the layer will grow in a highly strained state. Beyond a critical thickness, however, such a strained layer becomes unstable and relaxes through the nucleation and motion of dislocations, or through some other more complicated mechanism. Under ideal conditions, the relaxed layer provides a new crystalline substrate with a lattice constant differing from that of silicon, and therefore suitable for growing new kinds of devices. Not surprisingly, a great deal of attention has been focused on the problem of how a thin, highly strained layer can be made to relax in a well-controlled way [1,2].

An idealized relaxation process for a uniformly strained $Si_{1-x}Ge_x$ layer on Si(001) is illustrated in Fig. 1. Dislocation loops are nucleated and grow by glide [Fig. 1(b)]. As the threading arms T move outward on the glide plane, misfit dislocations M are left behind in the interface [or at the top and bottom interfaces in the case of the capped layer shown in Fig. 1(b)]. To the degree to which just enough dislocations are nucleated on the various glide planes, and all threading arms can propagate unimpeded to the edges of the layer, an array of misfit lines is created [Fig. 1(c)] which relieves the strain, with no threading arms remaining in the layer to degrade its properties. In actuality, neither the nucleation or the propagation of the dislocations is ideal, and a certain density of threading arms is invariably observed to remain after a layer has relaxed. Layers with threading-arm densities below 10^6 cm^{-2} are currently achieved using a strategy of graded layer growth, in which the Ge concentration is increased, gradually or stepwise, as the layer becomes thicker. Similarly high-quality results have been produced both by growing weakly graded layers at high (≈900 °C) temperatures using molecular beam epitaxy (MBE) [3] and rapid thermal chemical vapor deposition (RT-CVD) [4] and by growing more strongly graded layers at much lower (≈500 °C) temperatures using ultrahigh vacuum chemical vapor deposition (UHV-CVD) [5,6].

Observations of dislocation pileup structures in the substrates of relaxed epitaxial layers suggest that repetitive (Frank-Read or spiral) sources are an important nucleation mechanism, at least when the low temperature UHV-CVD process is used to grow the film. Thus it is tempting to consider a particular model of layer relaxation: One places a

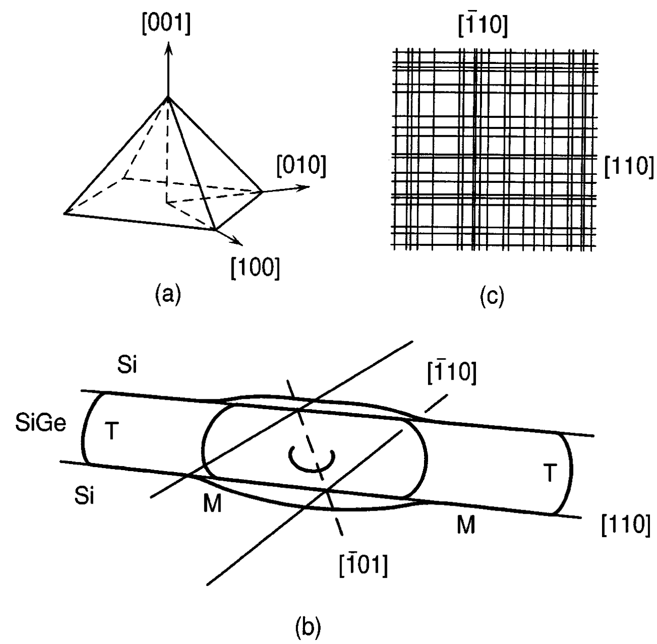

FIG. 1. (a) The pyramid shows the crystallographic directions appropriate to the fcc structure of Si. The base of the pyramid is parallel to the plane of the layer, which coincides with the (001) plane of the crystal. The faces of the pyramid define the {111} set of glide planes, while the edges coincide with the ⟨011⟩ set of allowed Burgers vectors. (b) Same-perspective view of two intersecting glide planes, $(1\bar{1}1)$ and (111), in the capped epilayer. A Frank-Read source located at the center of the $(1\bar{1}1)$ plane has produced two dislocations which are propagating away, and is in the process of growing a third loop. (c) Plan view of an idealized relaxed layer, showing the typical cross-hatched pattern of misfit dislocations that relieve the strain.

certain density of such sources into a strained layer, and lets the resulting system of dislocations evolve to its final state. Despite its attractive simplicity, the implications of this model are not clear. On the one hand, one can imagine that, as the threading-misfit complexes are produced, the threading arms will propagate outward unimpeded until all of the strain is relaxed. In this limit, the remanent threading-arm density will depend on the density of sources. In particular, a high density of sources will imply a high density of threading arms, unless some annihilation or recombination mechanism is invoked. On the other hand, one may suppose that, as the moving threading arms encounter dislocations produced by other sources, they experience strong local forces which lead to immobilization. For sufficiently low source densities, the remanent density of threading arms would then presumably be determined by the dislocation interactions. Since strong interactions between arbitrarily configured dislocations have not previously been accessible to investigation, it has not been clear which of these limits is more to the point, or, indeed, whether the model itself is sufficiently realistic to be useful. An intriguing sidelight is provided by the observation of elaborate, characteristically organized structures (Fig. 2) deep in the unstressed substrate when the low-temperature UHV-CVD process is used to grow the film [6]. Although the significance of these structures has been a matter of some controversy, we shall assume that they are a by-product of the layer relaxation processes, and should therefore be predicted by a realistic model.

The strong interactions that dislocations are likely to experience are conveniently divided into two categories. On the one hand, a threading arm propagating on its glide plane is certain to encounter misfit dislocations left behind on *intersecting* (crossed) glide planes. Such interactions have recently been investigated [7]. Here we focus on the quite different situation which arises when threading arms propagating on one glide plane have close encounters with dislocations moving on a *parallel* plane. In the limit where threading arms can propagate for long distances, this kind of encounter is likely to be experienced by every dislocation, and may be the mechanism which accounts for the existence of remanent threading dislocations.

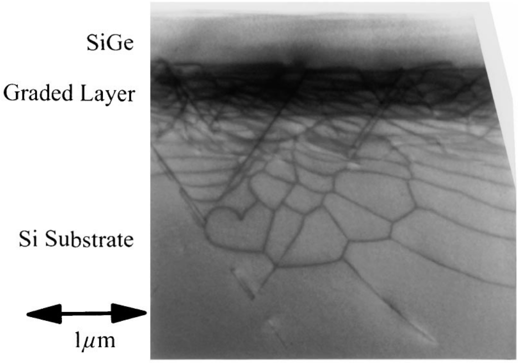

FIG. 2. [110] cross-sectional TEM picture of a graded SiGe layer grown on Si(100) by UHV-CVD at a temperature of 550 °C. The top SiGe layer contains 30% Ge.

Numerical simulations were carried out using a program that implements the full three-dimensional Peach-Koehler formalism [8] on a parallel computer. The force acting to move a dislocation element $d\vec{l}$ in the glide plane is $(b_i \sigma_{ij} n_j)(\hat{n} \times d\vec{l})$, where $\vec{b}$ is the Burgers vector, σ is the stress tensor, and $\hat{n}$ is the glide plane normal. The stress tensor includes stresses due to the applied strain, stresses generated by the presence of dislocations, and additional corrections arising from the presence of boundaries (such as the layer surfaces). For a uniformly strained, isotropic epitaxial layer lying in the xy plane, $\sigma_{xx} = \sigma_{yy} = 2\epsilon_0 \mu(1 + \nu)/(1 - \nu)$, where ϵ_0 is the strain, μ is the shear modulus, and ν is Poisson's ratio. This field provides the mechanism driving the motion of the dislocations. We avoid dealing with the difficult free-surface problem by considering the symmetrical capped layer shown in Fig. 1(b). It remains to determine the contributions to the stress tensor generated by the dislocations themselves. For an isotropic crystal, the contribution to the stress at $\vec{r}$ due to an element $d\vec{l}$ at $\vec{r}\,'$ is

$$d\sigma_{\alpha\beta} = (\mu/4\pi R^3)[(\vec{b} \times \vec{R})_\alpha dl_\beta + (\vec{b} \times \vec{R})_\beta dl_\alpha] + [\mu/4\pi(1 - \nu)R^5](d\vec{l} \times \vec{b})_\gamma \times [R^2(\delta_{\alpha\gamma}R_\beta + \delta_{\beta\gamma}R_\alpha - \delta_{\alpha\beta}R_\gamma) - 3R_\alpha R_\beta R_\gamma], \quad (1)$$

where $\vec{R} = \vec{r} - \vec{r}\,'$, $\delta_{\alpha\beta}$ is the Kronecker delta, and the index γ is summed over. The form (1) can be integrated analytically over a straight line segment. To evaluate σ_{ij} at a particular point, the dislocations are approximated as a chain of sufficiently short straight segments, and the relevant expression summed numerically. Additional information concerning the method of calculation can be found in Ref. [7], and a detailed exposition of the computational approach and physical approximations underlying these simulations is in preparation.

We first describe the computed behavior of two threading arms encountering each other [9]. Since they are oppositely oriented, they attract. Since, however, they are on different glide planes, and cross slip is not considered here, they cannot reconnect. The outcome is a bound state which immobilizes the two dislocations as seen in the center of Fig. 3(a). This result is hardly surprising, and the idea that two dislocations can immobilize each other in this way is well appreciated by workers in the field. What makes the numerical approach more interesting, even on this simple level, is that it provides detailed information of the type required to develop realistic models of the layer-relaxation process. This is illustrated by Fig. 4, which shows the calculated properties of the binding process for a 100 nm thick capped layer. We see that, for a given glide-plane separation, dislocations will

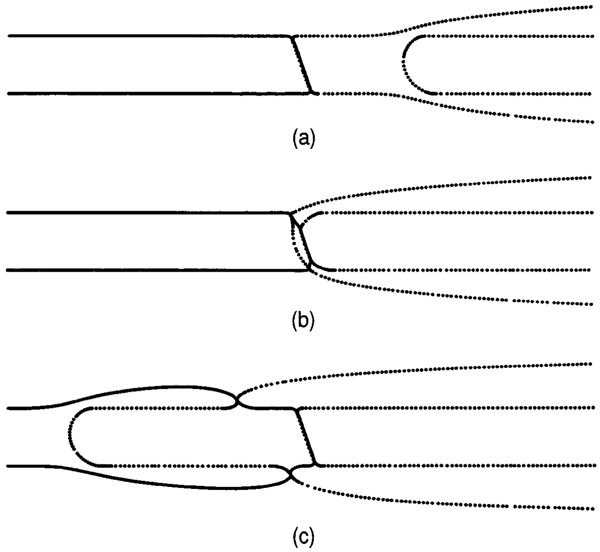

FIG. 3. Encounter of a third dislocation with a bound dislocation pair, time increasing from (a) to (c). This particular calculation was done on a 100 nm layer, with glide planes spaced eight glide-plane spacings apart, and $\epsilon_0 = 0.009$. One glide-plane spacing equals 0.326 nm. The view is along the $[\bar{1}10]$ direction. The dislocation on the plane in front is shown as a solid line; the one on the back plane is dotted. The top and bottom interfaces are not shown, but their location is obvious. The high quality of the computation can be judged from the fact that the dots are the actual mesh points used in the calculation.

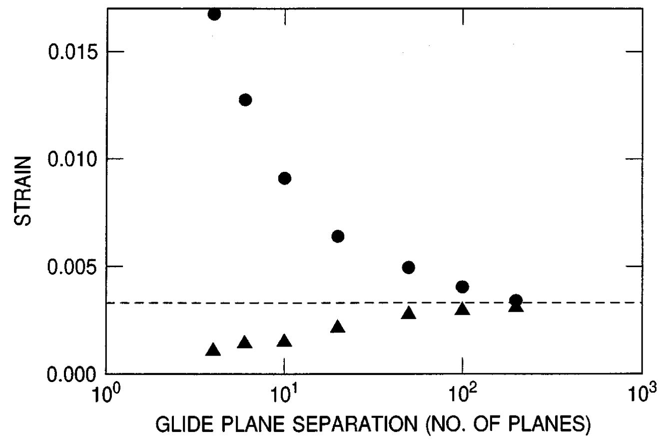

FIG. 4. Limits of trapping in a 100 nm capped layer. The circles represent the values of the strain above which no trapping occurs, while the triangles represent the values below which the bound state is pulled apart by the line tension. The dashed line is the computed critical strain for which an isolated threading arm is stationary.

pass by each other without binding if the applied stress driving their motion is greater than a certain value. As the separation increases, this binding limit decreases rapidly, and becomes only a few percent of the critical stress once the separation becomes comparable to the layer thickness. More unexpectedly, perhaps, we find that there is also a *lower* limit to the applied stress for which binding occurs: If the stress is reduced below the critical stress, a point is reached where the line tension pulling the threading arms backwards overcomes their attractive interaction, and the two dislocations are pulled apart.

Some general aspects of layer relaxation can be deduced from Fig. 4. At high stress levels, only lines that pass very near each other (compared to the layer thickness) will bind. Although the trapping range increases as the stress is lowered towards the critical stress, the trapping process itself becomes weaker and more subject to small fluctuations in the local stress levels. Thus, as a highly strained layer relaxes, it will pass from a regime dominated by short-range encounters producing strongly bound states to a more complicated regime dominated by long-range interactions resulting in weakly bound states which may feel the effects of several dislocations at once, and which are easily disturbed by other perturbations such as the effects arising from misfits on the intersecting glide planes.

An entirely new kind of information, illustrative of the qualitative new insights that numerical experiments can provide, is illustrated in Fig. 3. Suppose that a second threading arm produced by a Frank-Read source on the back plane approaches the bound pair as in Fig. 3(a). Our calculations show that as it propagates to the left, this new dislocation pushes the initial one on the back plane into the unstrained regions. As it approaches the bound pair, it repels the dislocation on its own glide plane, but attracts the one on the front plane [Fig. 3(b)]. Eventually, the initial dislocation on the back plane is pushed forward [Fig. 3(c)] and moves on, while the incoming dislocation binds in turn with the one left behind on the front glide plane. The dislocation which was displaced continues to propagate on the back plane unless it in turn encounters one coming in the other direction on the front plane. In this event a second bound state is formed. Figure 3(c) exhibits another unexpected new feature—the formation of locally bound sections where the misfits that have been pushed into the unstrained regions pass near each other. At these crossing points, the dislocations arrange themselves into locally antiparallel states.

To our knowledge, the simple mechanism depicted in Fig. 3 has not previously been identified. Its apotheosis is illustrated in Fig. 5, which depicts a structure created by two Frank-Read sources situated some distance apart on parallel glide planes. The repeated application of the mechanism is seen to create a sequence of bound threading-arm pairs in the strained layer, accompanied by an elaborate and beautiful structure in the unstrained regions. This structure has the nature of an elastic network, the nodal points being regions where there is binding across the two glide planes.

The importance of our finding is best illustrated by comparing Fig. 5 with the transmission electron microscopy (TEM) image of Fig. 2 showing actual substrate structures typical of those frequently observed. Although real structures cannot be expected to match the idealized computer simulation exactly, there can be little doubt that much of the observed substrate structure consists of elastic networks formed by Frank-Read sources on parallel glide planes. Aside from the striking qualitative similarity

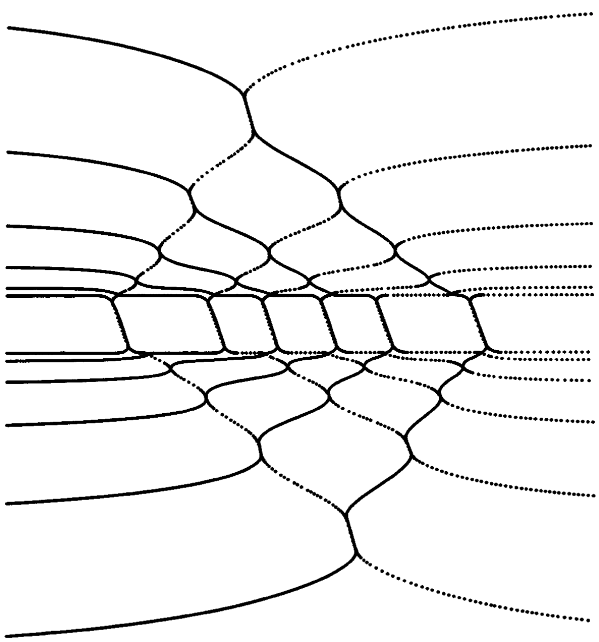

FIG. 5. Dislocation structure built by two Frank-Read sources on parallel glide planes. Threading arms are propagating in from both sides of the figure, and the structure results from the repetitive action of the mechanism illustrated in Fig. 3.

between observed and computationally predicted network patterns, the size scale of the observed networks (which is roughly proportional to the strained-layer thickness) is also in reasonable agreement with our predictions. Most of the remaining structure takes the form of simple pileups, and of corner pileups, which have been shown recently [7] to arise from the interaction of Frank-Read sources on *intersecting* glide planes. Historically, these pileup structures have been the exclusive focus of attention, while network patterns have been ignored. Our present results indicate that the networks are of equal significance, and (together with the results of [7]) demonstrate that essentially all of the striking structures observed in the substrates of high-quality buffer layers (at least in those grown by low temperature UHV-CVD) can be understood in terms of a low density of Frank-Read sources that emit dislocations which travel along the layer, and which interact strongly when they encounter each other. This model therefore appears to be the proper starting point for further studies.

Finally, it has not been clear if the other processes used to produce high-quality buffer layers involve relaxation mechanisms that differ in some important way from those which we have just ascribed to the low-temperature UHV-CVD process. In particular, the characteristic substrate structures exemplified by Fig. 2 have not been clearly identified for layers prepared by high-temperature MBE or RT-CVD. It is therefore very interesting to note that a predicted secondary (and perhaps more robust) signature of having Frank-Read sources interacting across parallel glide planes is the generation of sequences of bound dislocation pairs, threading the layer and stringing out along a glide direction with a spacing on the order of the layer thickness. These kinds of structures have, in fact, been shown to be plentiful in RT-CVD films (see particularly Figs. 4 and 5 of Ref. [4]). One is therefore encouraged to hope that the basic physical mechanisms that determine the remanent density of threading dislocations will not depend greatly on the process used to grow the layers.

To summarize, we have used numerical simulation to explore the strong interactions between threading dislocations approaching each other on parallel glide planes. It is found that for glide planes a certain distance apart, there is a range of strains over which the two dislocations bind in an immobile state. Above this range, the dislocations move past each other; below it, they unbind and retreat towards their original source. The range of applied strain over which two dislocations are bound is large at small separations, but becomes negligible at separations comparable to the layer thickness. A bound pair can also be separated by the arrival of a third dislocation. In this case, the new arrival will displace its predecessor (which continues to move forward), and will in turn form a bound state with the dislocation left behind. Through this mechanism, repetitive dislocation sources on parallel glide planes will create a row of bound dislocation pairs in the layer, along with elaborate dislocation networks in the unstrained substrate. Both of these phenomena have been observed experimentally. Thus we conclude that the mechanism identified here is important for layer relaxation and accounts for much of the substrate patterns observed.

The authors gratefully acknowledge illuminating discussions with J. Tersoff and P. M. Mooney.

[1] P. M. Mooney, Mater. Sci. Eng. **R17**, 105 (1996).
[2] R. Beanland, D. J. Dunstan, and P. J. Goodhew, Adv. Phys. **45**, 87 (1996).
[3] E. A. Fitzgerald, Y. H. Xie, D. Monroe, P. J. Silverman, J. M. Kuo, A. R. Kortan, F. A. Thiel, and B. E. Weir, J. Vac. Sci. Technol. B **10**, 1807 (1992).
[4] G. P. Watson, E. A. Fitzgerald, Y. H. Xie, and D. Monroe, J. Appl. Phys. **75**, 263 (1994).
[5] B. S. Meyerson, K. J. Uram, and F. K. LeGoues, Appl. Phys. Lett. **53**, 2555 (1988).
[6] F. K. LeGoues, B. S. Meyerson, J. F. Morar, and P. D. Kirchner, J. Appl. Phys. **71**, 4230 (1992).
[7] K. W. Schwarz Phys. Rev. Lett. **38**, 4785 (1997).
[8] See, for example, J. P. Hirth and J. Lothe, *Theory of Dislocations* (Krieger Publishing, Florida, 1992).
[9] The parameters used in the calculations are those appropriate to Si_xGe_{1-x} on Si. Specifically, unit cell dimension $a = 5.65 \times 10^{-8}$ cm, shear modulus $\mu = 6.77 \times 10^{10}$ Pa, and Poisson ratio $\nu = 0.218$. Our conclusions are not sensitive to these values. The strain is related to the Ge concentration by $\epsilon \approx -0.042x$, although we have framed our discussion in terms of response to a positive strain. All calculations were done on 8 or 16 nodes of an IBM SP2 supercomputer.